Simulation of inelastic neutron scattering spectra using OCLIMAX

Y. Q. Cheng*, L. L. Daemen, A. I. Kolesnikov, A. J. Ramirez-Cuesta*

Neutron Scattering Division, Oak Ridge National Laboratory, Oak Ridge TN, 37831

Emails: chengy@ornl.gov, ramirezcueaj@ornl.gov

Abstract

Studying the vibration of atoms is of fundamental importance and can provide critical insight for the understanding of materials behavior, such as structure and phase transition, thermodynamics, and chemical reactions. The atomic vibration can be probed using vibrational spectroscopy with various incident particles such as photons, neutrons, or electrons. A major challenge when applying these techniques is often how to interpret the vibrational spectra, and how to make connections to the theory. To this end, methods that can simulate the spectra from atomistic models are highly desired. In this paper, we present a program developed for the simulation of inelastic neutron scattering spectra. It has many new and useful features that were not previously available, and will greatly facilitate the analysis and understanding of inelastic neutron scattering data.

Introduction

Inelastic neutron scattering (INS) is a powerful technique to measure atomic vibrations in materials, with some unique advantages over other spectroscopic methods. Unlike photons (x-rays or lasers), neutrons interact directly with nuclei, thus INS is a direct probe of the atomic dynamics with no selection rules. In addition, the energy and momentum of thermal neutrons are comparable to phonons, allowing measurement of the dynamical structure factor in a wide and relevant range for both energy transfer and momentum transfer (e.g., Brillouin zone sampling, phonon dispersion and phonon density of states). Neutrons also penetrate deep into the material, and deposit only a small amount of energy, such that neutron scattering is often considered a bulk, non-destructive probe. Apart from these experimental features, another advantage of INS is that its simulation is relatively straightforward, with rigorous theory established for the calculation of INS spectra from phonons (normal modes frequencies and polarization vectors). In computer simulation, the information on phonons can be obtained from either quantum or classical calculations, and the calculation of INS also takes experimental perspectives into consideration, such as the instrument geometry, resolution, nature of the sample, etc. This type of simulation is crucial in connecting theory and experiment, and in many cases it is required even for the interpretation of the experimental data. On the other hand, INS also provides one of the most stringent tests of theory (for example density functional theory, or DFT), as the model has to predict not only the correct structure but also the correct vibrational dynamics. Therefore, how to help researchers to perform INS simulations routinely is of great interest and importance in the neutron scattering community.

In this paper we present OCLIMAX, a program developed primarily for INS simulations of powder samples. The name derives from the initial code produced by Kearley and Tomkinson that was called CLIMAX.[1] CLIMAX used force field methods to fit the INS spectra of simple molecules, and its application is very limited. Later in 2002, Champion, Tomkinson, and Kearley produced the very first version of aCLIMAX (auntie-CLIMAX was the original name that was shortened to aCLIMAX).[2] aCLIMAX was able to produce INS spectrum from the output of DFT modeling, but the first incarnation was extremely slow. In 2004, Ramirez-Cuesta distributed the final version of aCLIMAX.[3] It was a Visual Basic interface that runs a series of subroutines compiled in Fortran 90. The main features of aCLIMAX include incoherent approximation to calculate low-temperature INS spectra for the TOSCA/VISION instruments,[4,5] calculation of combinations and overtones, as well as phonon wing calculations for single molecules. It was very fast and became the standard software for INS analysis for indirect geometry instruments. This version of aCLIMAX is still available on the web. OCLIMAX, with the O representing ORNL, has been coded from scratch, with many new features added to extend its applications in much broader field. Adding to the existing features of aCLIMAX, the OCLIMAX program now allows full calculation of INS spectra with coherent effects and temperature effects, for various INS instruments and arbitrary trajectories in the momentum and energy transfer (Q-ω) space. It also supports simulation for INS from single crystals as well as powder diffraction pattern. It can be operated as standalone application and run from scripts on large number of systems, making it possible to do high throughput analysis of INS data. The current version of OCLIMAX however does not perform simulation of magnetic neutron scattering, which tends to be more system/model-dependent and there have been other tools dedicated for such problems (e.g., SpinWave[6] and SpinW[7]). Different from the Monte Carlo ray tracing approach (MCViNE[8]), OCLIMAX calculates the dynamical structure factor directly from the phonon information. It also comes with a script to convert phonon calculation output files from various codes (e.g., VASP, CASTEP, Phonopy, CP2K, Gaussian, ORCA, NWChem) to the input files needed for INS calculation. The entire procedure can be as simple as two command lines. The program is released as a Docker[9] image (command line only) or within the ICEMAN[10] virtual machine (graphic interface, under development), which makes it completely self-contained and system/environment independent. All these are aimed to lower the barrier and eliminate steep learning curves for users, such that one can easily use the program to generate their own INS spectra to be compared with experimental data. In the following, we will discuss the method for INS calculation and demonstrate the main features of the program.

Theory

The fundamental (one phonon) excitation from coherent inelastic neutron scattering can be expressed as:[11]

$$S_{coh\pm1}(\boldsymbol{Q},\omega) = \frac{1}{2N}\sum_s \sum_{\boldsymbol{\tau}} \frac{1}{\omega_s}\left|\sum_d \frac{\bar{b}_d}{\sqrt{M_d}} \exp(-W_d)\exp(i\boldsymbol{Q}\cdot\boldsymbol{r}_d)\,(\boldsymbol{Q}\cdot\boldsymbol{e}_{ds})\right|^2 \times (n_s + \frac{1}{2} \pm \frac{1}{2})\delta(\omega \mp \omega_s)\delta(\boldsymbol{Q} \mp \boldsymbol{q} - \boldsymbol{\tau}) \quad (1)$$

where ω_s is the frequency (of mode s), M_d is the atomic mass (of atom d). $\boldsymbol{e}_{ds}$ is the polarization vector, $\boldsymbol{r}_d$ is the position of atom d in the unit cell. $\boldsymbol{q}$ is a wavevector of the phonon mode s and $\boldsymbol{\tau}$ is the corresponding vector in the reciprocal lattice (note that the summation is over all sampled modes in the Brillouin zone, and each mode s has its corresponding $\boldsymbol{q}$). $\exp(-W_d)$ is the Debye-Waller factor, which can be calculated as $W_d = \frac{\hbar}{4M_d N_q}\sum_s \frac{(\boldsymbol{Q}\cdot\boldsymbol{e}_{ds})^2}{\omega_s}(2n_s+1)$. b is the neutron scattering length (of atom d).

In a simpler form, the incoherent inelastic neutron scattering can be calculated as:[11]

$$S_{inc\pm 1}(\boldsymbol{Q},\omega) = \sum_d \frac{1}{2M_d}\left\{\bar{b}_d^2 - \left(\bar{b}_d\right)^2\right\} \exp(-2W_d) \sum_s \frac{|\boldsymbol{Q}\cdot\boldsymbol{e}_{ds}|^2}{\omega_s}(n_s + \frac{1}{2} \pm \frac{1}{2})\delta(\omega \mp \omega_s) \quad (2)$$

where $\bar{b}_d^2 - \left(\bar{b}_d\right)^2$ is defined as the incoherent scattering cross-section of atom *d*.

When the material contains elements with large incoherent scattering cross-section, or the crystal structure is relatively complicated (i.e., large unit cell with small Brillouin zone), incoherent approximation often works well for polycrystalline or powder samples. To calculate the dynamical structure factor under incoherent approximation, one may replace the incoherent scattering cross-section in Eq. (2) with the total scattering cross-section. It is obvious that for incoherent scattering, the total intensity is a direct summation of the contribution from each atom. In the following equations we will focus on the contribution from a generic atom *d*, and omit the subscript *d* for simplicity.

At low temperature, Eq. (2) can be reduced to a much simpler form,[12] in which the fundamental and overtones from mode *s* (for any specific atom) can be expressed as:

$$S(\boldsymbol{Q}, n\omega_s) = \frac{(\boldsymbol{Q}\cdot\boldsymbol{U}_s)^{2n}}{n!} exp[-(\boldsymbol{Q}\cdot\boldsymbol{U}_{\boldsymbol{total}})^2] \quad (3)$$

where $\boldsymbol{U}_s = \sqrt{\frac{\hbar}{2M\omega_s}}\boldsymbol{e}_{ds}$ is essentially the zero-point displacement of the atom due to mode *s*, and $\boldsymbol{U}_{\boldsymbol{total}}$ is the total displacement of the atom with all modes. This simple equation governs the spectra measured at TOSCA/VISION on hydrogen containing materials at base temperature.

For powder samples, an important procedure is to perform orientational averaging over the vector *Q*. In OCLIMAX, the original *k* mesh used for phonon calculation is expanded to beyond the first Brillouin zone, and then for certain *Q* the orientational averaging is performed numerically on the modes falling within the designated *ΔQ* (bin size) at *Q*. For incoherent scattering or incoherent approximation, which has a simpler mathematical expression, powder averaging can be performed analytically (with approximations), as derived for aCLIMAX[12]. We will not repeat the derivation here, but the final equations are given below.

For one-quantum events (fundamental):

$$S(Q,\omega_s) = \frac{Q^2 tr(\boldsymbol{B}_s)}{3}\exp(-Q^2\alpha_s) \qquad \text{where} \qquad \alpha_s = \frac{1}{5}\left[tr(\boldsymbol{A}) + \frac{2(\boldsymbol{B}_s{:}\boldsymbol{A})}{tr(\boldsymbol{B}_s)}\right] \tag{4}$$

For two-quantum events (combination):

$$S\big(Q,\omega_{s,t}\big) = \frac{Q^4}{15}\left[tr(\boldsymbol{B}_s)tr(\boldsymbol{B}_t) + \boldsymbol{B}_s{:}\boldsymbol{B}_t + \boldsymbol{B}_t{:}\boldsymbol{B}_s\right]\exp(-Q^2\beta) \qquad \text{where} \qquad \beta = \frac{tr(\boldsymbol{A})}{3} \tag{5}$$

In the above equations:

$$\boldsymbol{B}_s = \boldsymbol{U}_s\boldsymbol{U}_s^T = \begin{bmatrix} U_{s1}U_{s1} & U_{s1}U_{s2} & U_{s1}U_{s3} \\ U_{s2}U_{s1} & U_{s2}U_{s2} & U_{s2}U_{s3} \\ U_{s3}U_{s1} & U_{s3}U_{s2} & U_{s3}U_{s3} \end{bmatrix} \qquad \text{and} \qquad \boldsymbol{A} = \textstyle\sum_{\boldsymbol{s}} \boldsymbol{B}_s \tag{6}$$

$$\boldsymbol{X}{:}\boldsymbol{Y} = \textstyle\sum_{\boldsymbol{i}=\boldsymbol{1}}^{\boldsymbol{3}} \sum_{\boldsymbol{j}=\boldsymbol{1}}^{\boldsymbol{3}} X_{ij}Y_{ij} \tag{7}$$

It should be noted that in Eq. (5), the two-quantum events are calculated by considering all possible combinations of the fundamental modes and evaluating their contributions to the intensity. It is accurate but also time-consuming. The expression for three-quantum events can also be derived, but it is not computationally feasible except for small systems. A more commonly used approach, which is much more efficient and usually sufficient, is to calculate the higher order excitations (multiphonons) by convolution:[13]

$$S_n(\omega) = \int_{-\infty}^{\infty} S_1(\omega-\omega')\, S_{n-1}(\omega')d\omega' \tag{8}$$

Note that in general the convolution on $S_n(\omega)$ must be done at atomic level, before applying the scattering cross-section and Debye-Waller factor.

In some cases where the crystal structure is unknown or too complicated, one would like to mimic the solid spectrum based on single molecule simulations. In this case the intermolecular vibrations (or external modes) are treated as phonon wings.[3,12]

$$S_{Origin} = S_{Total} \cdot \exp(-\boldsymbol{Q}^2 \cdot \boldsymbol{U}_{Ext}^2) \tag{9}$$

$$S_{Wing} = S_{Total} - S_{Origin} \tag{10}$$

where S_{Total} is the total scattering intensity due to a particular vibrational mode, S_{Origin} is the intensity still at the original frequency of the mode when external/intermolecular motions are considered, and is the intensity that migrates into the phonon wing due to external/intermolecular motions. The key information from the above Eqs. (9-10) is that the total intensity from a molecular mode is redistributed between the origin and the wing that follows it. The balance is determined by vibrational amplitude of the external modes. Details on the theory of wing calculation can be found in literature[3,12].

Finally, to simulate the INS spectra (or *Q*-*ω* map), one needs to apply proper resolution to the calculated intensity. Gaussian resolution function is used in OCLIMAX, with the standard deviation or full-width-half-maximum (FWHM) determined according to the geometry and other parameters of the beamline/instrument. For example, a generic equation for the FWHM on a direct geometry instrument is[14]

$$\frac{d(\hbar\omega)}{E_i} = 2\sqrt{\left(1+\frac{L_2}{L_3}\left(\frac{v_f}{v_i}\right)^3\right)^2\left(\frac{dt_m}{t_1}\right)^2 + \left(1+\frac{L_1+L_2}{L_3}\left(\frac{v_f}{v_i}\right)^3\right)^2\left(\frac{dt_c}{t_1}\right)^2 + \left(\frac{v_f}{v_i}\right)^4\left(\frac{dL_3}{L_3}\right)^2} \tag{11}$$

where E_i is the incident energy, L_1 is the distance from the moderator to the Fermi chopper, L_2 is the distance from the chopper to the sample, L_3 is the distance from the sample to the detector, t_1 is the neutron time-of-flight to the chopper, v_i and v_f are the initial and final speed of the neutrons, dt_m is the time spread of the moderator, dt_c is the time window through the Fermi chopper, and dL_3 is the path length uncertainty associated with the finite size of sample/detector.

For an indirect geometry instrument such as VISION or TOSCA, it is found that the energy-dependent resolution can be approximately described by:

$$\sigma = 0.25 + 0.005 \times \Delta E + 0.0000001 \times \Delta E^2 \tag{12}$$

where ΔE is the energy transfer, and σ is the standard deviation of the Gaussian function (both in the unit of wavenumber). Note that for Gaussian distribution, FWHM is about 2.3548σ. In most cases these equations work sufficiently well, and when properly parameterized, they do follow the measured resolution closely.[15]

In general, if the instrument parameters in Eqs (11) and (12) are not known, the E and Q resolution in OCLIMAX can be set as parameterized polynomial with the energy/momentum transfer as the variable. The parameters can be obtained, for example, by fitting the actual/measured resolution of the instrument.

Program

The OCLIMAX program and its manual (including installation and user guide) can be found on the web.[16] OCLIMAX requires an .aclimax (incoherent approximation simulation only) or .oclimax (required by coherent simulation) file, as well as an optional .params file to run. The .aclimax/.oclimax file contains information on the atomic structure, isotope, neutron scattering cross-sections, and phonons, and the .params file contains parameters defining the simulation (if different from the default). The .aclimax/.oclimax file can be obtained from the output file(s) of a phonon calculation (e.g., using Phonopy), by running the conversion script provided in the program. Currently the script supports output files from CASTEP, VASP (either directly from VASP or through Phonopy), CP2K, Quantum Espresso, Phonopy, ORCA, DMol3, NWChem, etc. In the .params file, users can specific how the calculation should be done. The default setup is for TOSCA/VISION spectrum simulation. One can modify the .params file to include combinations and overtones (up to a desired order), temperature effect, coherent effect, isotope substitution, and phonon wing calculation. The users can select to simulate the full $S(Q,\omega)$ map, or certain sampling trajectories corresponding to a (real or virtual) direct or indirect geometry instrument. A detailed explanation of the input parameters can be found in the manual. The program is currently distributed as a Docker image, allowing it to run on various platforms with minimum environment dependence. For most calculations with optimized phonon sampling density and parameters, it should take no more than a few minutes to finish. Also distributed on the website is a script to generate quick plot for visualization of the calculated spectra (pclimax.py).

Examples

We present here a few examples to demonstrate the main features of OCLIMAX. The phonon calculations in these examples were performed with CASTEP[17], VASP[18], and Phonopy[19], and the results were converted to the input files for OCLIMAX using the provided script. Since the phonon calculation itself is not the focus of this paper, the technical details are not listed here but can be found in several related publications.[20]

The first example is toluene, which has a molecular formula of C_7H_8 and the neutron scattering is thus dominated by the incoherent scattering from hydrogen. Toluene is a molecular crystal at low temperature. To reproduce the VISION spectrum of toluene measured at 5 K (Fig. 1), one can start with a single molecule model that calculates the internal vibrational modes. After converting to INS spectrum with OCLIMAX, one can see that most of the peaks above 20 meV are reproduced reasonably well. However, certain features in the spectrum do not agree with experiment, e.g. the low energy part below 20 meV, the background intensity between peaks, the additional peaks that are either not observed or much weaker in experiment (32 meV, 70 meV, 118 meV etc.), and peak splitting at 122 meV. The next level of approximation is adding the wing calculation, which essentially convolves the single molecule spectrum with an approximated phonon density of states describing the external modes. The convolution is expected to produce background intensities between the peaks, as indeed observed in Fig. 1, but the other issues cannot be addressed unless the intermolecular interaction is properly considered. This calls for a full crystal calculation, which results in a greatly improved agreement with the experiment. Specifically, the low energy band is now captured; the additional peaks at 32/70/118 meV are much weaker (almost invisible), the peak splitting at 122 meV is reproduced, and even the relative intensity of peaks (e.g., the two peaks near 90 meV) is corrected. The final agreement is excellent, demonstrating the capability of OCLIMAX to simulate VISION spectrum.

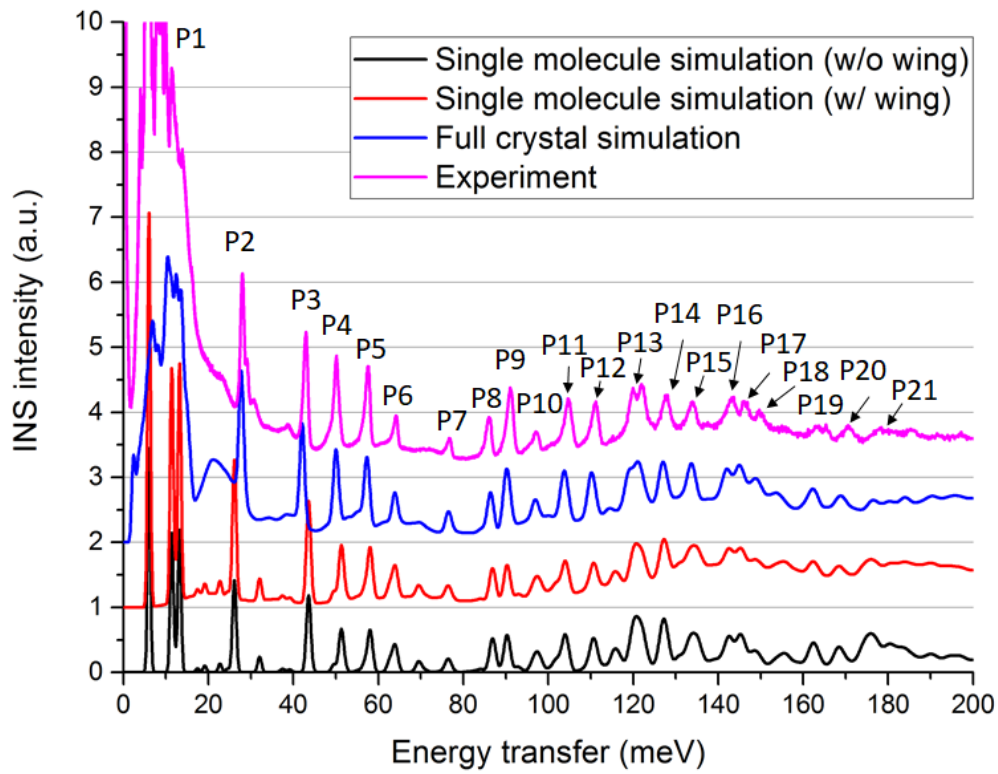

Figure 1. VISION INS spectrum of toluene at 5K, in comparison with OCLIMAX calculation at various approximation levels.

Once an agreement is achieved between experiment and simulation, the observed peaks in the INS spectra can be fully and unambiguously assigned. In this case of toluene, peaks are assigned in Table 1 below, with the corresponding modes illustrated in Fig. 2.

Table 1. Peak assignment for the toluene spectrum in Fig. 1. Since some modes are hybrid/mixed, the description is only meant to reflect the main character of the mode.

Label	Energy transfer (meV)	Visualization (Fig. 2)	Description
P1	~10	M1	-CH_3 torsion, translation/libration
P2	28	M2	Ring-CH_3 out-of-plane deformation
P3	43	M3	Ring-CH_3 in-plane deformation
P4	50	M4	Ring out-of-plane deformation
P5	57.5	M5	Ring out-of-plane deformation
P6	64	M6	Ring in-plane deformation
P7	76.5	M7	Ring in-plane deformation
P8	86	M8	=C-H out-of-plane deformation
P9	91	M9	=C-H out-of-plane deformation
P10	97	M10	Ring in-plane deformation
P11	104.5	M11	=C-H out-of-plane bending
P12	111	M12	=C-H out-of-plane bending
P13	121	M13	-CH_3 rocking/wagging

		M14	=C-H out-of-plane bending
P14	128	M15 M16	Ring stretching $-CH_3$ rocking/wagging
P15	134	M17	Ring stretching
P16	143	M18	=C-H in-plane deformation
P17	146	M19	=C-H in-plane deformation
P18	150	M20	=C-H in-plane deformation
P19	164	M21	Ring-CH_3 stretching
P20	170.5	M22	=C-H in-plane deformation
P21	179	M23, M24	C=C stretching, CH_3 umbrella

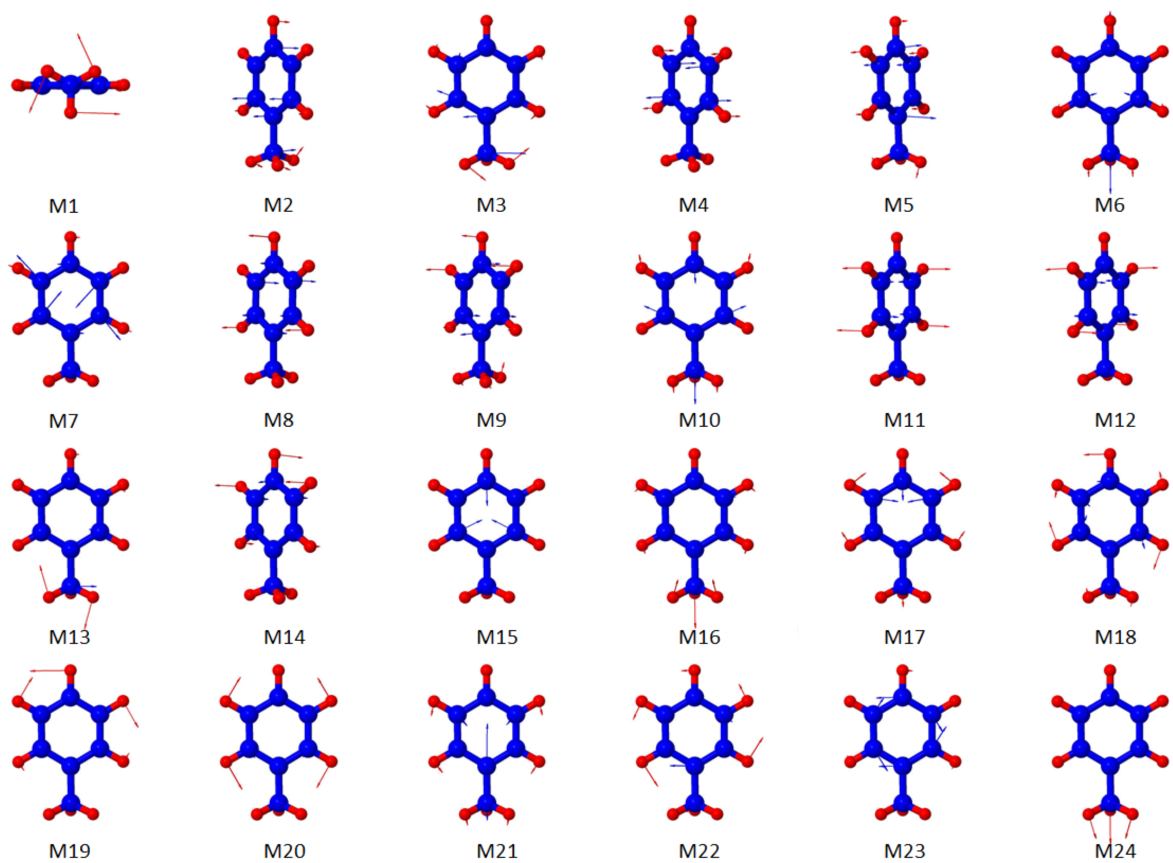

Figure 2. Visualization of the vibrational modes corresponding to the peak assignment in Tab. 1. For clarity a single molecule is used to illustrate the internal modes. Color scheme: blue for carbon and red for hydrogen.

We further test a larger system with more complicated structure, a metal-organic-framework (MOF), ZIF-8. The measured and simulated spectra are compared in Fig. 3, with the unit cell shown in the inset (data from original publication[21]). The overall agreement is very good. There are minor differences such as the position of certain peaks, but they are more likely to be caused by the DFT phonon calculation itself, rather than the INS calculation.

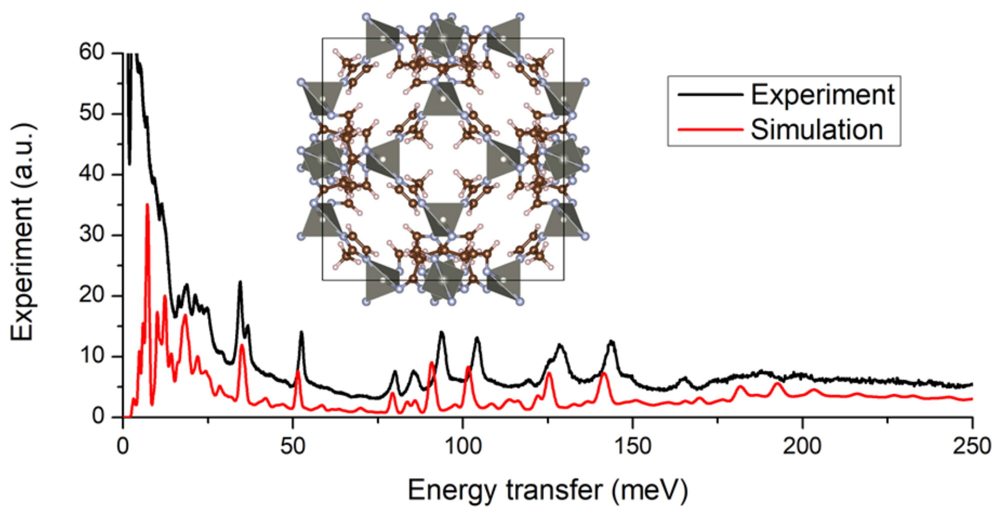

Figure 3. VISION spectrum of ZIF-8 at 5 K, in comparison with OCLIMAX calculation (inset shows the unit cell of the MOF).

The next example is magnesium hydride (MgH_2), in which we expect significant contribution from higher order excitations (multiphonon, or combination/overtone). As seen in Fig. 4, indeed one cannot reproduce the measured INS spectrum without considering the higher order contributions. OCLIMAX allows users to calculate higher order spectra through convolution. The calculation time for higher order terms linearly scales with the highest order requested. Although there is no hard limit on the highest order in OCLIMAX, in most cases a calculation of up to order 10 is sufficient. The users also have the option to calculate the 2nd order excitation in a more accurate way, but it takes significantly longer time than the simple convolution.

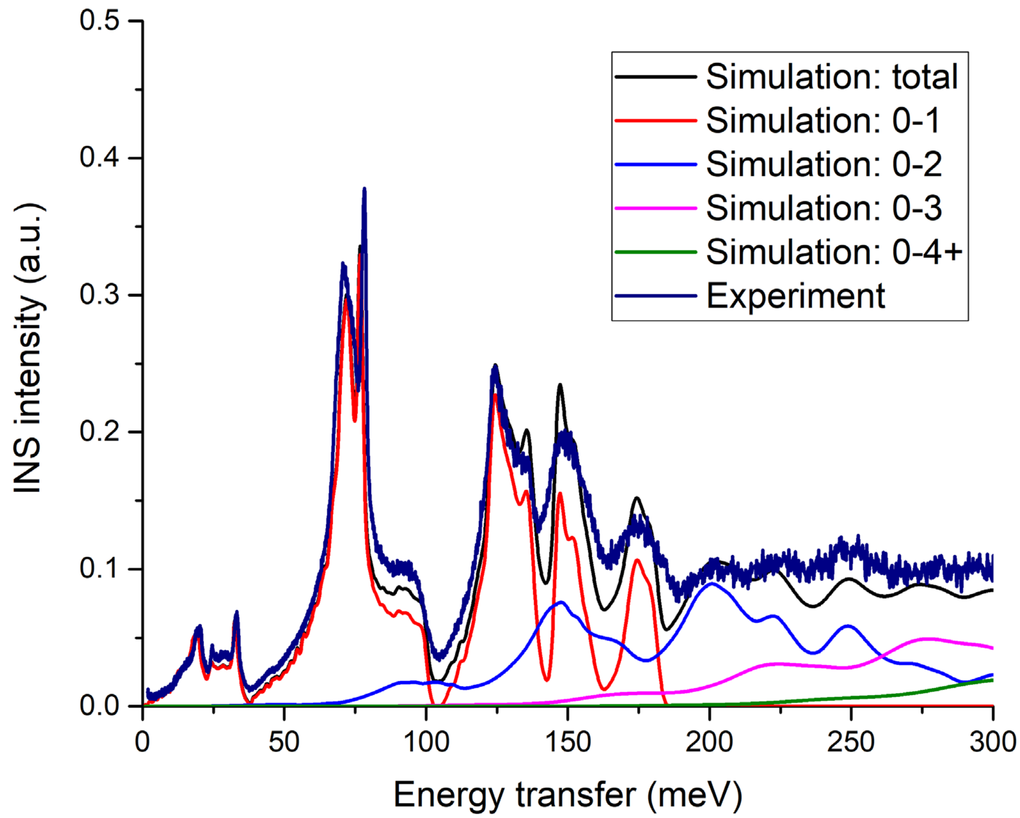

Figure 4. VISION spectrum of MgH_2 at 5 K, in comparison with OCLIMAX calculation (the total intensity is decomposed into contribution of each order).

A new feature OCLIMAX offers is the calculation of INS at finite temperatures. This is achieved by including the temperature population (or vibrational amplitude) of the phonons in the equations, also taking consideration of detailed balance. An example of this feature in $LiAlH_4$ is shown in Fig. 5 (original publication on the experiment[22]). The temperature dependence of the spectra is nicely reproduced by the program. It should be noted that to properly evaluate the temperature effect, treatment of the low energy modes is critical since they become populated first and the most when temperature is increased. This has an effect not only in the low energy range of the spectrum, but also in the higher energy part through combinations with the higher energy modes (as demonstrated by the peak broadening and the elevated background intensity). For this purpose, one would need a very accurate calculation of the low energy modes, sufficiently dense sampling in the Brillouin zone, and evaluation of the combination modes up to certain order. All these putting together can be difficult to achieve, and this is often the challenge for higher temperature INS calculations, especially for soft materials (where the potential contribution from quasi-elastic scattering and its combination with phonons will make it even more complicated).

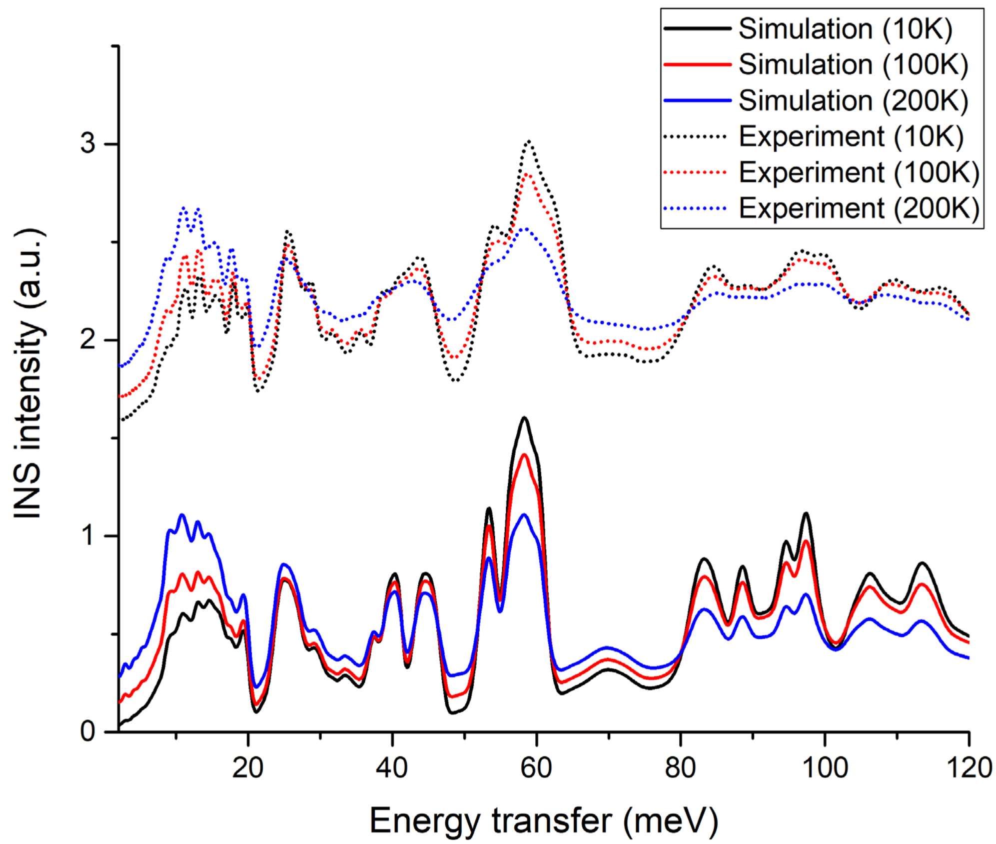

Figure 5. Temperature dependent VISION spectra of $LiAlH_4$, in comparison with OCLIMAX calculations at the corresponding temperatures.

Another major new feature of OCLIMAX is the capability to calculate coherent inelastic scattering, from both powders and single crystals, and this can be done for a generic neutron spectrometer, direct geometry or indirect geometry, with fully adjustable instrument geometry parameters. An example of graphite powder, measured at SEQUOIA spectrometer[23] and simulated with OCLIMAX using SEQUOIA parameters, is shown in Fig. 6. A strong coherent scattering is expected in this sample, as demonstrated by the dispersion curves observed in the SEQUOIA spectra, even for a powder sample. OCLIMAX nicely reproduces the coherent effect.

(a)

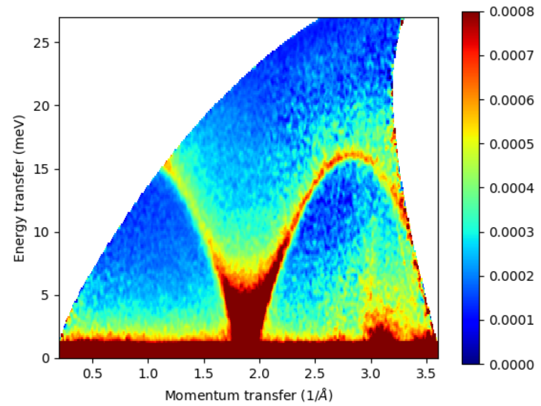

Energy transfer (meV)
Momentum transfer (1/Å)
0.0008
0.0007
0.0006
0.0005
0.0004
0.0003
0.0002
0.0001
0.0000

(d)

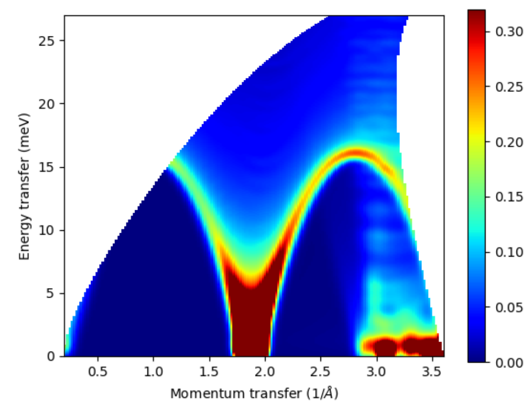

Energy transfer (meV)
Momentum transfer (1/Å)
0.30
0.25
0.20
0.15
0.10
0.05
0.00

(b)

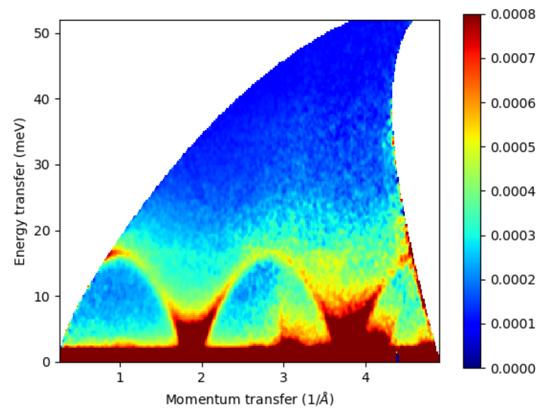

Energy transfer (meV)
Momentum transfer (1/Å)
0.0008
0.0007
0.0006
0.0005
0.0004
0.0003
0.0002
0.0001
0.0000

(e)

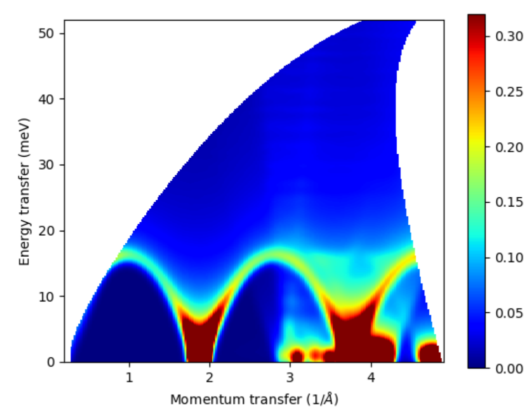

Energy transfer (meV)
Momentum transfer (1/Å)
0.30
0.25
0.20
0.15
0.10
0.05
0.00

(c)

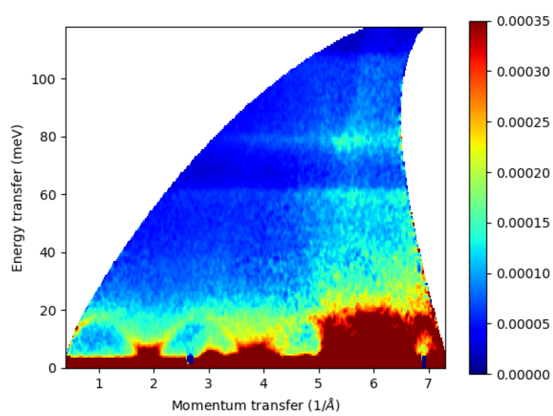

Energy transfer (meV)
Momentum transfer (1/Å)
0.00035
0.00030
0.00025
0.00020
0.00015
0.00010
0.00005
0.00000

(f)

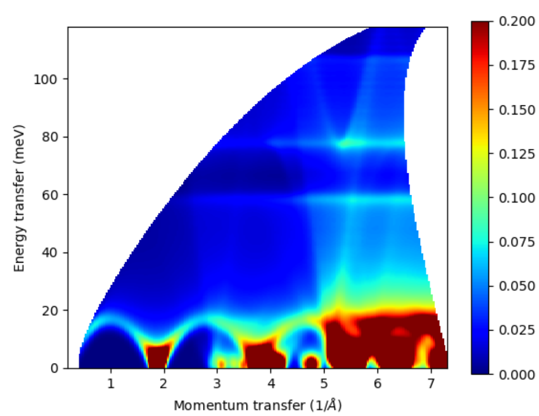

Energy transfer (meV)
Momentum transfer (1/Å)
0.200
0.175
0.150
0.125
0.100
0.075
0.050
0.025
0.000

Figure 6. Graphite powder measured at SEQUOIA with Ei of (a) 30 meV, (b) 55 meV, and (c) 125 meV, at 293K. The corresponding simulations at the same temperature with OCLIMAX are shown in (d), (e), and (f). Note that the elastic peak is not simulated.

Such strong coherent effect in graphite also manifests itself in the VISION spectrum. It has been noticed, but not well understood, that the measured graphite spectrum from TOSCA/VISION does not agree well with simulation[12]. Since the previous simulations were all performed with incoherent approximation, the coherent effect was not included. With OCLIMAX we can now perform a full calculation including the coherent effect. It is clearly seen in Fig. 7 that the discrepancy observed before (especially around 30 meV) was mainly due to coherent effect.

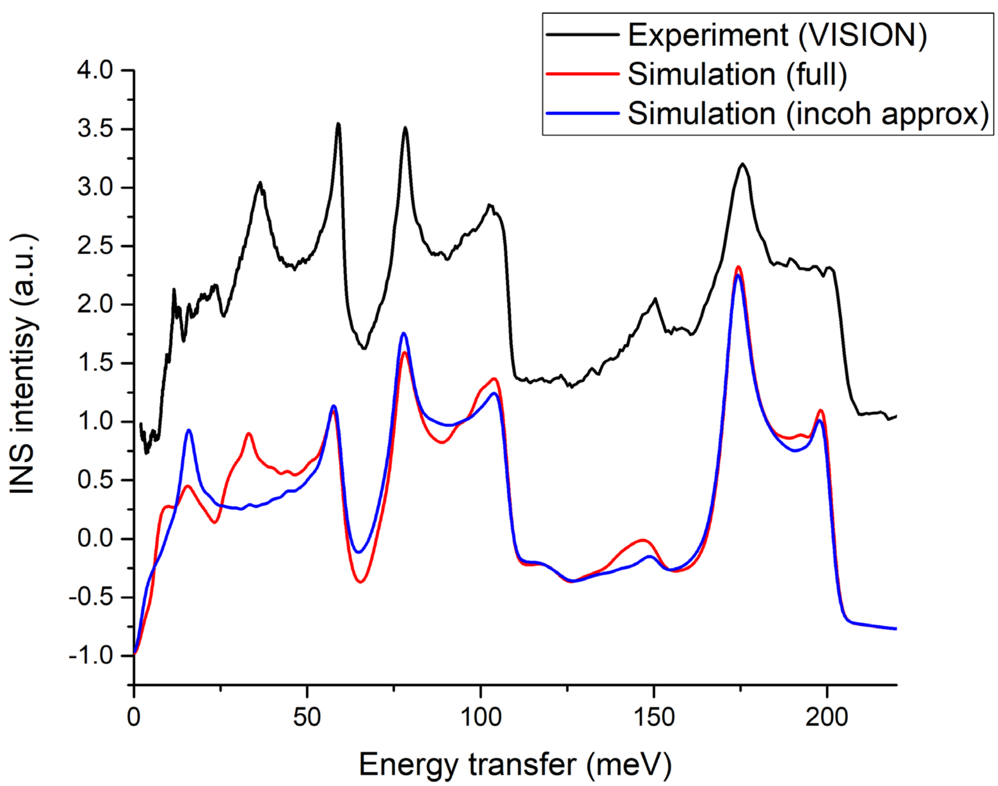

Figure 7. VISION spectrum of graphite powder measured at 5 K, in comparison with OCLIMAX calculation under incoherent approximation and with full consideration of the coherent effect.

Application

The goal of performing an INS simulation is often to extract information that is not directly available from the experimental data alone, or to obtain insight connecting fundamental theory with experimental observations. In this section we present an example of how OCLIMAX can be used to resolve an apparent contradiction between theory and experiment.

The maximum intensity in $S(Q,\omega)$ along certain energy cut occurs at Q_{max}, which can be determined by

$$\left.\frac{\partial S(Q,\omega)}{\partial Q}\right|_{Q=Q_{max}} = 0 \qquad (13)$$

For incoherent scattering and under isotropic assumption, one can simplify Eq. (3) as:

$$S(Q,n\omega_s) = \frac{\left[\frac{Q^2 tr(\boldsymbol{B}_S)}{3}\right]^n}{n!} exp\left(-\frac{Q^2 tr(\boldsymbol{A})}{3}\right) \qquad (14)$$

Plugging Eq. (14) into Eq. (13), it can be solved that

$$Q_{max} = \sqrt{\frac{3n}{tr(\boldsymbol{A})}} \qquad (15)$$

The implication of this equation is, assuming the harmonic, incoherent, and isotropic approximations are valid, Q_{max} should be independent of the energy for fundamental modes (and its value is only determined by the total mean-square displacement), this is because $tr(\boldsymbol{A})$ corresponds to the summation of $tr(\boldsymbol{B}_s)$ for all modes, and therefore its value is no longer dependent on the mode of interest. For combinations and overtones, Q_{max} should follow a $\sqrt{n}$

dependence where n is the order of the combination/overtone. This is an interesting conclusion and its validity should be confirmed with experiment.

Figure 8(a) shows the $S(Q,\omega)$ of ice-Ih measured at SEQUOIA. In this system the assumptions for Eq. (15) to hold can be considered valid, at least for the purpose of this study. However, it is clearly seen that Q_{max} has a strong energy dependence for all peaks, e.g. Q_{max} is about 8 Å^{-1} for the librational band (around 90 meV), while it is at ~14 Å^{-1} for the OH stretch modes (around 410 meV). Without further information, it is difficult to explain this apparent contradiction.

The OCLIMAX simulation of up to 10 orders of multiphonon excitations is shown in Fig. 8(b), which matches the experiment data in Fig. 8(a) very well. The advantage of simulation is that one can easily and unambiguously separate the contributions from fundamentals and overtones. In Fig. 8(c) we plot the contribution from fundamental modes only. It can be seen that in this plot Q_{max} is no longer sensitive to energy, consistent with theoretical prediction. Figure 8(d) highlights the extracted Q_{max} values in Figs. 8(a-c). For the total $S(Q,\omega)$, OCLIMAX reproduced the experimental observation (i.e., strong energy dependence of Q_{max}) very well, but when only fundamental contribution is considered, the energy dependence becomes very weak and negligible, consistent with theory. The apparent contradiction with theory in Fig. 8(a) is caused by contributions of higher order excitations (combinations of the fundamental modes and mostly strong acoustic peak at ~7 meV) – this overlap shifts the peak position in Q to a higher value (i.e., higher Q_{max}).

It should be noted that for fundamental modes, Eq. (15) is only valid when $\alpha_s = \frac{1}{5}\left[tr(\boldsymbol{A}) + \frac{2(\boldsymbol{B}_S:\boldsymbol{A})}{tr(\boldsymbol{B}_S)}\right] \approx \frac{1}{3}[tr(\boldsymbol{A})]$, see Eq. (4). In other words, we need to have $\frac{(\boldsymbol{B}_S:\boldsymbol{A})}{tr(\boldsymbol{B}_S)} \approx \frac{1}{3}[tr(\boldsymbol{A})]$. This approximation only holds well when the system is isotropic, i.e., the incoherent INS spectra measured from different directions on a single crystal should be similar. Ice-Ih is one of such isotropic systems, as demonstrated previously by Li[24]. It is possible that in certain anisotropic systems, Q_{max} of the fundamental modes has an intrinsic dependence on energy/mode, which is beyond the scope of the current study.

(a)

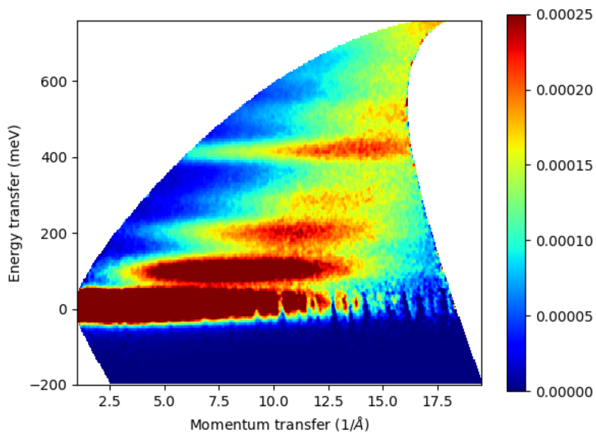

(b)

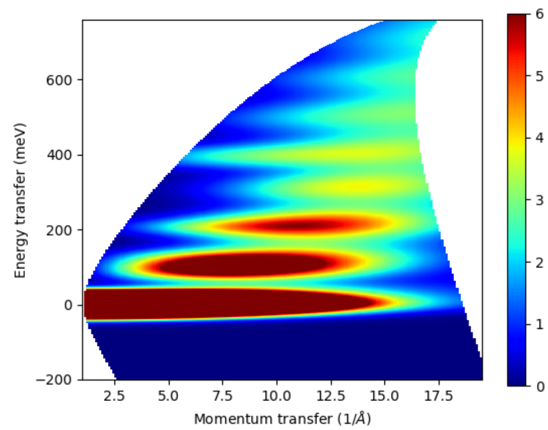

(c)

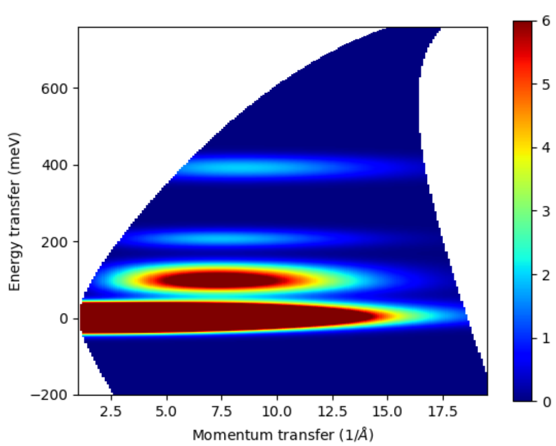

(d)

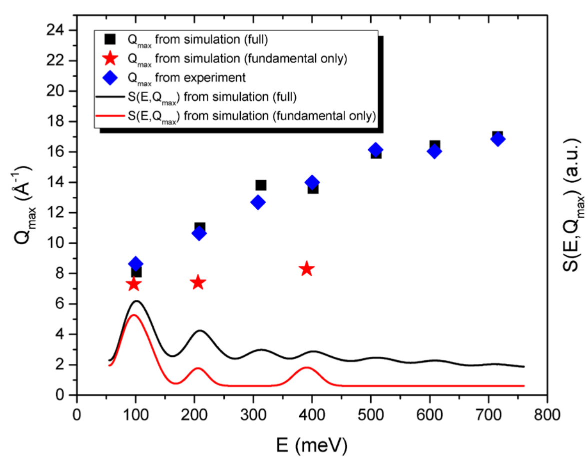

Figure 8. (a) INS spectrum of Ice-Ih at 6 K measured at SEQUOIA with Ei of 800 meV. (b) Corresponding simulation with OCLIMAX including excitations up to 10 orders. (c) Simulation with OCLIMAX for fundamentals only. (d) Comparison of Q_{max} for total $S(Q,\omega)$ (both

experiment and simulation), as well as the contribution from fundamental modes only (simulation).

Conclusion

In this paper we present OCLIMAX, a program for simulation of inelastic neutron scattering directly from phonon frequencies and polarization vectors. The program can perform wing calculation, solve higher order excitations (combinations/overtones), calculate INS at finite temperature, and generate spectra for any generic instrument geometry (direct and indirect, with fully adjustable instrument parameters). Moreover, it goes beyond the incoherent approximation and can perform full calculations including coherent effects. The program is released with a script that converts output files from various popular phonon calculation software (VASP, CASTEP, CP2K, Phonopy, Gaussian, ORCA, DMol3, NWChem, etc.) to the input files needed by OCLIMAX. An optional parameter file can be appended to define the calculation. The standard output data is in csv format. The users can also select to generate a restart file (in binary format), SPE file (for DAVE[25]) or (neutron weighted) phonon density of states. Overall it is much more powerful than its previous version aCLIMAX, as well as the recently developed ABINS algorithm[26] in Mantid.[27] We believe this is a much-needed tool for the inelastic neutron scattering community. OCLIMAX will continue to be developed, and updated docker images can be obtained easily by following the user manual.[16]

Acknowledgements

Neutron scattering experiments were conducted at ORNL's Spallation Neutron Source, which is supported by the Scientific User Facilities Division, Office of Basic Energy Sciences (BES), U.S. Department of Energy (DOE), under Contract No. DE-AC0500OR22725 with UT Battelle, LLC. The computing resources were made available through the VirtuES and the ICEMAN projects, funded by Laboratory Directed Research and Development program and Compute and Data Environment for Science (CADES) at ORNL.

References

[1] Kearley, G.J. A review of the analysis of molecular vibrations using INS. *Nucl. Instrum. Methods Phys. Res. A.* **1995**, *354*, 53-58.

[2] Champion, D.; Tomkinson, J.; Kearley, G. a-CLIMAX: a new INS analysis tool. *Appl. Phys. A*. **2002**, *74*, s1302–s1304.

[3] Ramirez-Cuesta, A.J. aCLIMAX 4.0.1, The new version of the software for analyzing and interpreting INS spectra. *Comput. Phys. Commun.* **2004**, *157*, 226–238.

[4] Parker, S.F.; Fernandez-Alonso, F.; Ramirez-Cuesta, A.J.; Tomkinson, J.; Rudic, S.; Pinna, R.S.; Gorini, G.; Castañon, J.F. Recent and future developments on TOSCA at ISIS. *J. Phys.: Conf. Ser.* **2014**, *554*, 012003.

[5] VISION website. https://neutrons.ornl.gov/vision (accessed February 5, 2019).[6] SpinWave website. http://www-llb.cea.fr/logicielsllb/SpinWave/SW.html (accessed February 5, 2019).

[7] Toth S.; Lake, B. Linear spin wave theory for single-Q incommensurate magnetic structures. *J. Phys.: Condens. Matter.* **2015**, *27*, 166002.

[8] Lin, J.Y.Y.; Smith, H.L.; Granroth, G.E.; Abernathy, D.L.; Lumsden, M.D.; Winn, B.; Aczel, A.A.; Aivazis, M.; Fultz, B. MCViNE – An object oriented Monte Carlo neutron ray tracing simulation package. *Nucl. Instrum. Methods Phys. Res. A*. **2016**, *810*, 86–99.

[9] Docker website. https://www.docker.com/ (accessed February 5, 2019).

[10] Integrated Computational Environment for the Modeling and Analysis of Neutrons

[11] Squires, G.L. *Introduction to the Theory of Thermal Neutron Scattering*; Dover Publications: New York, 1997.

[12] Mitchell, P.C.H.; Parker, S.F.; Ramirez-Cuesta, A.J.; Tomkinson, J. *Vibrational Spectroscopy with Neutrons*; World Scientific: Singapore, 2011.

[13] Fultz, B.; Kelley, T.; Lin, J.; Lee, J.D.; Delaire, O.; Kresch, M.; McKerns, M.; Smith, H. Experimental Inelastic Neutron Scattering with a Chopper Spectrometer, 2016. Springer-Verlag Web Site. http://www.its.caltech.edu/~matsci/btfgrp/Inelastic_Neutron_Book.pdf (accessed February 5, 2019).

[14] Abernathy, D.L.; Stone, M.B.; Loguillo, M.J.; Lucas, M.S.; Delaire, O.; Tang, X.; Lin, J.Y.Y.; Fultz, B. Design and operation of the wide angular-range chopper spectrometer ARCS at the Spallation Neutron Source, *Rev. Sci. Instrum*. **2012**, *83*, 015114.

[15] Seeger, P.A.; Daemen, L.L.; Larese, J.Z. Resolution of VISION, a crystal-analyzer spectrometer, *Nucl. Instrum. Methods Phys. Res. A*. **2009**, *604*, 719.

[16] OCLIMAX website. https://sites.google.com/site/ornliceman/download (accessed February 5, 2019).

[17] Clark, S.J.; Segall, M.D.; Pickard, C.J.; Hasnip, P.J.; Probert, M.J.; Refson, K.; Payne, M.C. First principles methods using CASTEP, *Zeitschrift fuer Kristallographie.* **2005**, *220*, 567-570.

[18] VASP website. https://www.vasp.at/ (accessed February 5, 2019).

[19] Togo, A.; Tanaka, I. First principles phonon calculations in materials science, Scr. Mater. **2015**, *108*, 1-5.

[20] VISION publication list. https://neutrons.ornl.gov/vision/publications (accessed February 5, 2019).

[21] Casco, M.E.; Cheng, Y.Q.; Daemen, L.L.; Fairen-Jimenez, D.; Ramos-Fernandez, E.V.; Ramirez-Cuesta, A.J.; Silvestre-Albero, J. Gate-opening effect in ZIF-8: First experimental proof using inelastic neutron scattering. *Chem. Commun*. **2016**, *2*, 3639-3642.

[22] Sato, T.; Ramirez-Cuesta, A.J.; Daemen, L.L.; Cheng, Y.Q.; Tomiyasu, K.; Takagi, S.; Orimo, S.I. Hydrogen release reactions of Al-based complex hydrides enhanced by vibrational dynamics and valences of metal cations. *Chem. Commun.* **2016**, *52*, 11807-11810.

[23] Granroth, G.E.; Kolesnikov, A.I.; Sherline, T.E.; Clancy, J.P.; Ross, K.A.; Ruff, J.P.C.; Gaulin, B.D.; Nagler, S.E. SEQUOIA: a newly operating chopper spectrometer at the SNS. *J. Phys.: Conf. Ser.* **2010**, *251*, 12058.

[24] Li, J.C. Inelastic neutron scattering studies of hydrogen bonding in ices, *J. Chem. Phys*. **1996**, *105*, 6733.

[25] Azuah, R.T.; Kneller, L.R.; Qiu, Y.; Tregenna-Piggott, P.L.W.; Brown, C.M.; Copley, J.R.D.; Dimeo, R.M. DAVE: A Comprehensive Software Suite for the Reduction, Visualization, and Analysis of Low Energy Neutron Spectroscopic Data, *J. Res. Natl. Inst. Stan. Technol*. **2009**, *114*, 341.

[26] Dymkowski, K.; Parker, S.F.; Fernandez-Alonso, F.; Mukhopadhyay, S. AbINS: the modern software for INS interpretation. *Physica B: Condens. Matter*. **2018**, *551*, 443-448.

[27] Arnold, O.; Bilheux, J.C.; Borreguero, J.M.; Buts, A.; Campbell, S.I.; Chapon, L.; Doucet, M.; Draper, N.; Ferraz Leal, R.; Gigg, M.A.; Lynch, V.E.; Markvardsen, A.; Mikkelson, D.J.; Mikkelson, R.L.; Miller, R.; Palmen, K.; Parker, P.; Passos, G.; Perring, T.G.; Peterson, P.F.; Ren, S.; Reuter, M.A.; Savici, A.T.; Taylor, J.W.; Taylor, R.J.; Tolchenov, R.; Zhou, W.; Zikovsky, J. Mantid - Data analysis and visualization package for neutron scattering and μSR experiments. *Nucl. Instrum. Methods Phys. Res. A*. **2014**, *764*, 156-166.

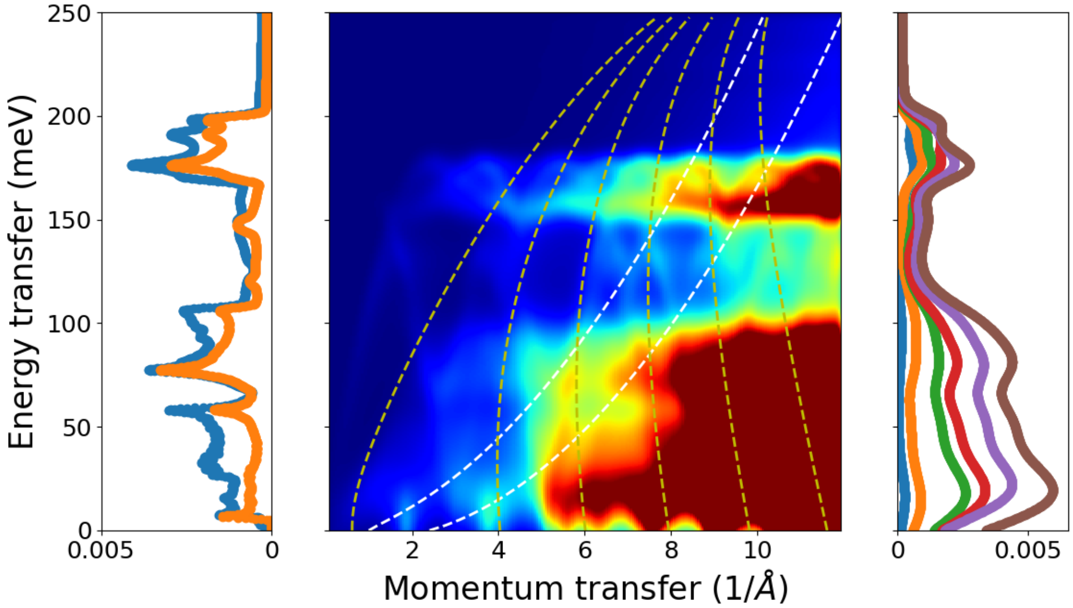

For Table of Contents Only